Journal of Quantitative Spectroscopy & Radiative Transfer 299 (2023) 108520

Contents lists available at ScienceDirect

Journal of Quantitative Spectroscopy & Radiative Transfer

journal homepage: www.elsevier.com/locate/jqsrt

# Satellite characterization of global stratospheric sulfate aerosols released by Tonga volcano

P. Bernath[a,b,c,*], C. Boone[b], A. Pastorek[a], D. Cameron[c], M. Lecours[b]

[a] Department of Chemistry and Biochemistry, Old Dominion University, Norfolk, VA, USA
[b] Department of Chemistry, University of Waterloo, Waterloo, ON, Canada
[c] Deparment of Physics, Old Dominion University, Norfolk, VA, USA

ARTICLE INFO

*Article history:*
Received 20 December 2022
Revised 2 February 2023
Accepted 3 February 2023
Available online 5 February 2023

*Keywords:*
Volcanic eruptions
Fourier transform spectroscopy
Stratosphere
Sulfate aerosols
Infrared remote sensing
Satellite

ABSTRACT

Large volcanic eruptions create an enhanced layer of sulfate aerosols in the stratosphere. These sulfuric acid droplets persist for many months, altering the climate and stratospheric chemistry. Sulfate aerosols scatter sunlight back to space, cooling the surface of the Earth and absorb outgoing thermal radiation, heating the stratosphere. The calculation of the climate impact of sulfate aerosols depends on their physical properties such as droplet size and chemical composition. These properties are not well known, and this uncertainty contributes to the errors in climate model predictions. Here we derive the first empirical formula that predicts the composition of stratospheric sulfate aerosols from volcanic eruptions from the air temperature and water vapor pressure. Measurements of atmospheric infrared transmittance of the Hunga Tonga-Hunga Ha'apai sulfate aerosol plume by the Atmospheric Chemistry Experiment (ACE) satellite were analyzed to determine composition (weight percent of sulfuric acid) and median particle radius. These data are supplemented by measurements of the Raikoke and Nabro eruptions. Our analysis allows the properties of volcanic aerosols in the stratosphere to be predicted reliably in atmospheric models.



## 1. Introduction

Stratospheric sulfate aerosols from volcanic eruptions play an important role in the physical and chemical processes in the Earth's atmosphere [1]. They have a strong impact on climate by absorbing and scattering both incoming and outgoing radiation [1]. Stratospheric aerosols cool the surface of the Earth by scattering incoming solar radiation and heat the stratosphere by absorbing outgoing thermal radiation. For example, the large 1991 volcanic eruption of Mt. Pinatubo in the Philippines resulted in a reduction of the average surface temperature of the Earth[4] by 0.4 K [2]. In addition to their climate impact, these aerosols affect stratospheric chemistry; for example, the Mt. Pinatubo eruption decreased stratospheric ozone by 3–4% [3]. Sulfate aerosols are seed particles for the formation of Polar Stratospheric Clouds (PSCs), which are responsible for the Antarctic ozone hole [1]. The stratospheric circulation is also altered by large tropical eruptions as the stratospheric heating increases the pole-to-equator temperature gradient resulting in a stronger Arctic polar vortex [4]. Aerosols are essential components of climate models, but to date their contributions are incomplete and have large error bars [5]. Improved climate predictions depend on improved aerosol physical and chemical parameters.

The Hunga Tonga-Hunga Ha'apai volcano (hereafter just Tonga) erupted violently on 15 January 2022 with an energy release [6] comparable to the largest atmospheric nuclear test explosion. The Tonga eruption reached a record altitude of 57 km in the mesosphere based on the analysis of visible satellite images [7,8]. The Tonga volcano is located underwater near 20.54°S latitude and 175.38°W longitude. This underwater eruption injected a large quantity [9,10] of water vapor into the stratosphere, which has a cooling effect in the enhanced water layer [11,12].

The amount of $SO_2$ injected into the stratosphere was a relatively modest 0.41 ± 0.02 Tg compared to ~1 Tg from the 2019 Raikoke eruption and 17 Tg emitted by the 1991 Pinatubo eruption [9]. The enhanced water vapor caused the $SO_2$ lifetime to be decreased by a factor of two by increasing the concentration of the OH radical [13]. $SO_2$ was therefore rapidly (12-day lifetime) converted to sulfate aerosol [13].

Stratospheric sulfate aerosols from the Tonga eruption were observed by several satellite, balloon-borne and ground-based instruments. Kloss et al. [14] used laser light scattering to measure particle size distributions in the Tonga plume with a balloon-borne instrument on the 23 and 26 January 2022 at La Réunion (21.1°S, 55.3°E). Lidar measurements of the sulfate plume were also made

* Corresponding author.
*E-mail address:* pbernath@odu.edu (P. Bernath).

https://doi.org/10.1016/j.jqsrt.2023.108520
0022-4073/

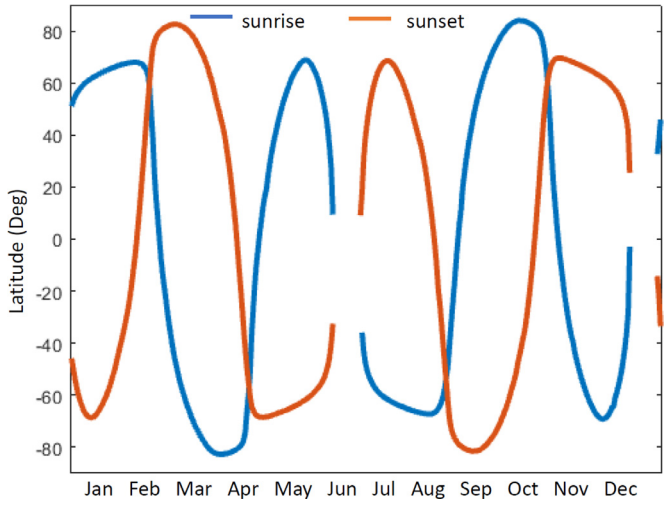


**Fig. 1.** Location of ACE measurements. Latitude distribution of ACE occultations for 2021. This latitude distribution is approximately the same for each year.

from the Maïdo observatory on La Réunion at about the same time. Nadir images of the Tonga plume based mainly on the IASI (Infrared Atmospheric Sounding Interferometer) instrument were also provided. Taha et al. [15] used the OMPS LP (Ozone Monitoring and Profiler Suite, Limb Profiler) to track the aerosol plume in space and time for about 150 days. Taha et al. [15] found that the Tonga eruption had the largest stratospheric aerosol optical depth since the 1991 eruption of Mt Pinatubo.

The climate impact of stratospheric sulfate aerosols is determined by several factors including particle number density, particle size distribution, average particle size, and particle composition. Lacis et al. [16] showed that particle size is an important factor and large particles (effective radii greater than 2 $\mu$m) can cause global surface heating, rather than cooling. Composition (weight percent of sulfuric acid) directly affects the extinction of sunlight and the absorption of thermal radiation from the Earth. This composition [1] is typically assumed to be 75% by weight of $H_2SO_4$ although we will show that the composition varies from about 45% to 79%.

As illustrated by Fig. 1a) of Boone et al. [17], composition has a dramatic effect on infrared aerosol extinction, so this assumption of 75% introduces a serious systematic error in stratospheric heating by sulfate aerosols. Optical constants of sulfate aerosols used to model scattering in the visible region also depend on composition [18] and again an assumed composition introduces systematic errors in climate models as well as lidar, limb scattering, solar occultation and nadir retrievals of sulfate aerosol properties. Our empirical function for aerosol composition can generate more realistic values and improve the accuracy of these analyses.

The deliberate formation of sulfate aerosols, for example by using aircraft to directly inject $SO_2$ or $H_2SO_4$ into the stratosphere, has been suggested in order to temporarily counteract global warming [19,20]. Prediction of the radiative effects of such geoengineering requires accurate knowledge of the composition and size of sulfate aerosols.

The ACE (Atmospheric Chemistry Experiment) satellite [21] has been making extensive observations of the Tonga eruption and we focus on the characterization of Tonga sulfate aerosols with the ACE-FTS (ACE Fourier Transform Spectrometer). ACE-FTS records infrared atmospheric transmittance spectra in the limb geometry using the Sun as a light source. "Residual" spectra are calculated by removing the retrieved spectral features due to gas phase molecules, leaving the spectra of aerosols and clouds [17,22]. For the stratospheric sulfate aerosols, we determine median particle size and composition, and derive a general empirical equation that predicts the composition of stratospheric sulfate aerosols from volcanic eruptions based on ambient atmospheric conditions.

## 2. Methods

The ACE satellite [21] was launched by NASA in August 2003 and is still operating with little degradation in performance. The primary instrument is a high-resolution Fourier transform spectrometer operating in the 750–4400 $cm^{-1}$ (2.2–13.3 $\mu$m) spectral region. The ACE-FTS uses the Sun as a light source and measures atmospheric transmittance spectra during sunrise and sunset in the limb geometry (solar occultation). There are also 2 solar imagers that provide atmospheric extinction at 0.525 and 1.02 $\mu$m.

ACE-FTS spectra are processed on the ground [23] to provide concentration profiles as a function of altitude for 44 gaseous molecules [24] for version 4.1/4.2. The absorption features due to these molecules can be removed from the spectra to create "residual" spectra that contain broad features due to cloud and aerosol particles [22]. These residual spectra contain some artefacts, for example from molecules such as $HNO_3$ for which the experimental line lists are incomplete. Thus, each spectrum is divided by a suitable reference spectrum that does not contain the volcanic plume but does contain background sulfate aerosol contributions. The background sulfate aerosol contributions in these reference spectra are removed by fitting. The final, corrected residual spectrum therefore has artefacts largely removed, and sulfate contributions from both the background and the volcanic eruption.

Simulation of these characteristic spectra can provide information on composition, particle size and particle shape. For example, transmittance spectra of Polar Stratospheric Clouds (PSCs) have shown that binary nitric acid and water particles (supercooled nitric acid, SNA) are common in addition to nitric acid trihydrate (NAT), supercooled ternary solutions of nitric acid and sulfuric acid (STS), and ice [25]. The sulfate aerosols from the Raikoke volcanic eruption have also been characterized using residual ACE-FTS spectra [17].

The retrieval of sulfate aerosol properties is described in detail by Boone et al. [17]. Briefly, the simulated transmission spectra were calculated using the Beer-Lambert equation

$$\tau = A\exp(-\sigma_{ext} N\ell) = A\exp(-\alpha\ell) \quad (1)$$

in which $\ell$ (cm) is the path length, $\alpha$ ($cm^{-1}$) is the extinction coefficient, $N$ is the particle concentration (particles/$cm^3$), $\sigma_{ext}$ ($cm^2$/particle) is the extinction cross section. The extinction coefficient $\alpha$ was calculated with the Oxford University Mie scattering code for spherical particles (http://eodg.atm.ox.ac.uk/MIE/index.html) and $A$ is a baseline parameter fitted to improve the agreement with ACE spectra.

The extinction cross section $\sigma_{ext}$ includes both absorption and scattering, and depends on wavenumber, particle size distribution and optical constants of the material at a particular temperature. The temperatures were fixed to the values from ACE-FTS version 4.1/4.2 retrievals [23]. A single lognormal particle size distribution was used (Eq. (2)) as defined by the particle density $N$, median radius $r_m$ and width $S$ (S is the distribution standard deviation $\sigma$ in ln(r) space, $\sigma = \ln(S)$).

$$n(r) = \frac{N}{\sqrt{2\pi}} \frac{1}{\ln(S)} \frac{1}{r} \exp\left[-\frac{(\ln r - \ln r_m)^2}{2\ln^2(S)}\right] \quad (2)$$

For sulfate aerosols, we fixed $S$ to 1.3 because the distribution width cannot be determined from infrared data alone. The value of 1.3 is based on some preliminary sulfate aerosol retrievals that included infrared ACE data and co-incident optical SAGE III/ISS extinction data for the Raikoke volcanic eruption. The aerosol path length is not known so the column density $N\ell$ (particles/$cm^2$) in the limb direction is determined in the fit. The optical constants

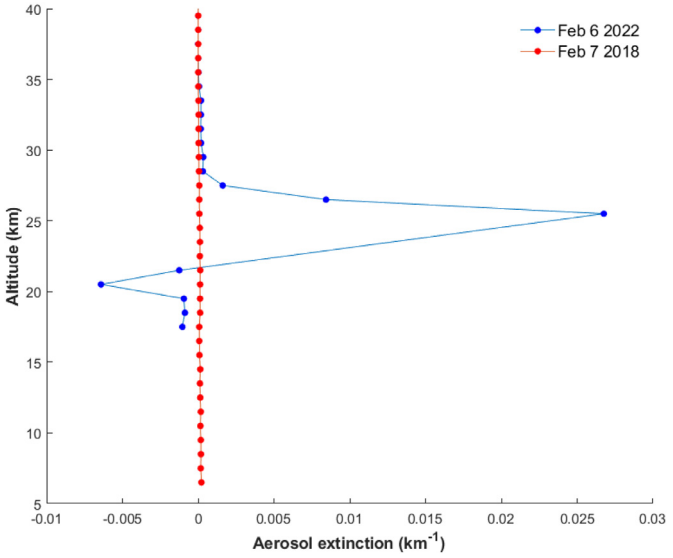


**Fig. 2.** Altitude profile of aerosol extinction. Aerosol extinction at 1.02 $\mu$m for ss99611 (ss for sunset and 99,611 is the orbit number from the start of the mission) on 6 February located at 19.85°S and 127.59°E. An extinction profile for a reference occultation (ss78053) recorded on 7 February 2018 without a volcanic plume is also displayed.

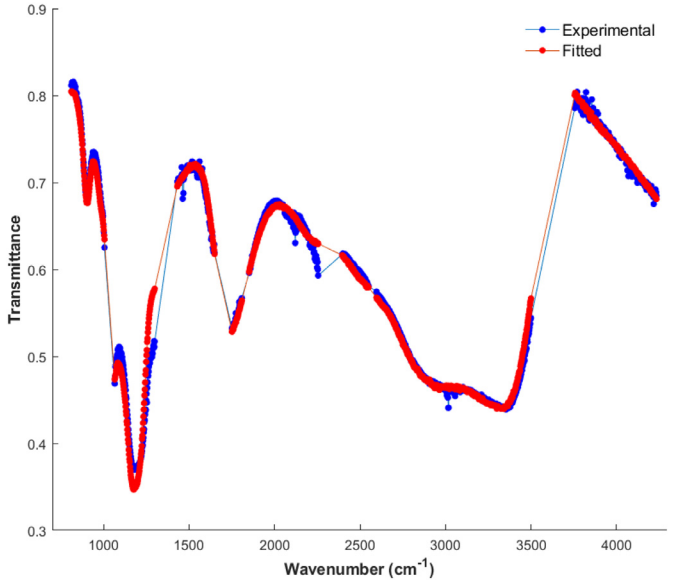


**Fig. 3.** Observed and calculated sulfate aerosol spectra. Tonga sulfate aerosol spectrum (blue) and fit (red) for ss99611 at 23.1 km altitude located at 19.85°S and 127.59°E recorded on 6 February 2022. The observed spectrum has been divided by the reference spectrum ss78053 to remove artifacts from incomplete removal of molecular lines.

for sulfuric acid in water are based on the values of Lund Myhre et al. [26]. The observed transmittance spectra are therefore fitted by adjusting 4 parameters, the baseline $A$, the median radius $r_m$, the composition (weight percent of $H_2SO_4$) and the column density, $N\ell$.

As discussed by Boone et al. [17], the fixed value of $S$, the width of the particle size distribution, has little effect on the retrieved value of the composition, which is determined by the infrared absorption features. However, the median radius is affected by the assumed value of $S$. For example, if the value of $S$ is set to 1.2 rather than 1.3 in the example in figures below, the median radius changes from 0.323 $\pm$ 0.002 $\mu$m to 0.365 $\pm$ 0.002 $\mu$m and the composition changes from 62.5 $\pm$ 0.2 wt% $H_2SO_4$ to 62.6 $\pm$ 0.2%. Therefore, the retrieved one standard deviation statistical error bars on composition are reasonable error estimates, but a more reasonable error for the retrieved radii is $\pm$0.04 $\mu$m.

In all cases, the aerosol temperature was assumed to be the retrieved air temperature at the tangent point [23]. To determine the effect of temperature on the retrieved parameters, the temperature was shifted by +5 K and −5 K (much larger than our temperature error of about 2 K) for a typical fit. Only the composition changed and in each case the shift was 0.2%, which is about half of the statistical error. The assumed temperature therefore has a negligible effect on the retrieved sulfate aerosol properties.

## 3. Results and discussion

ACE was measuring in Antarctica on 15 January 2022 when Tonga erupted. Fig. 1 shows the latitude distribution of ACE occultations for 2021, which is approximately the same each year. Typically, every day ACE measures up to 15 occultations in a longitude circle in each hemisphere. By 4 February the Southern Hemisphere occultations had moved northwards to about 28°S and encountered the Tonga plume.

The ACE satellite [21] also has a solar imager at a wavelength of 1.02 $\mu$m, from which the atmospheric extinction is retrieved. Fig. 2 shows this aerosol extinction as a function of altitude for ss99611 (ss for sunset and 99,611 is the orbit number from the start of the mission) on 6 February located at 19.85°S and 127.59°E. An extinction profile for a reference occultation (ss78053) without a volcanic plume is also displayed. Strong extinction in the plume caused a jump in pointing that resulted in a negative artifact below the peak in the ss99611 extinction profile. This figure shows that the aerosol cloud was so optically thick at about 24 km altitude that no sunlight at 1.02 $\mu$m penetrated the plume.

The corresponding residual stratospheric transmittance spectrum at 23.1 km altitude is provided in Fig. 3. The simulated spectrum (see Methods) shows that the plume is due to spherical sulfuric acid droplets with a median radius $r_m$ of 0.323 $\pm$ 0.002 $\mu$m, composition of 62.5 $\pm$ 0.2 wt% $H_2SO_4$, and column density of 5.2 $\pm$ 0.1 $\times$ $10^8$ particles/cm$^2$. The temperature was fixed to the retrieved value of 212.5 K [23] and the width of the monomodal lognormal particle size distribution $S$ was fixed to 1.3. As discussed above, the assumed temperature has a negligible effect on the retrieved parameters, but this assumed valued of $S$ introduces a systematic error of about 10% in the median radius. The retrieved properties for the occultations in the Tonga aerosol plume are provided in Supplementary Information Table 1. Reported uncertainties are random errors from least squares fitting and do not include systematic error contributions.

The latitude of the Tonga plume was tracked with the 1.02 $\mu$m ACE imager. During February 2022 the plume was located between 30°S and 10°N latitude and by April 2022 covered 40°S and 20°N (Fig. 4). By June 2022, the plume had reached Antarctica and in August (Fig. 5) extended from 25°N to within the Antarctic polar vortex, where Polar Stratospheric Clouds (PSCs) were observed along with sulfate aerosols. In August 2022, the plume was near 22 km altitude at the equator, but descended steadily to about 18 km at 60°S. The plume persisted and was present in October 2022 from 30°N to Antarctica. By late November 2022 the Tonga plume reached the Arctic at about 21 km in altitude and was still strongly present in Antarctica. Tonga stratospheric aerosols have therefore spread around the globe. Daily plots of atmospheric extinction from the 1.02 $\mu$m imager are available on the ACE website, https://ace.uwaterloo.ca/.

The composition of the Tonga aerosols was observed to depend on both temperature and water vapor pressure (Fig. 6). In order to

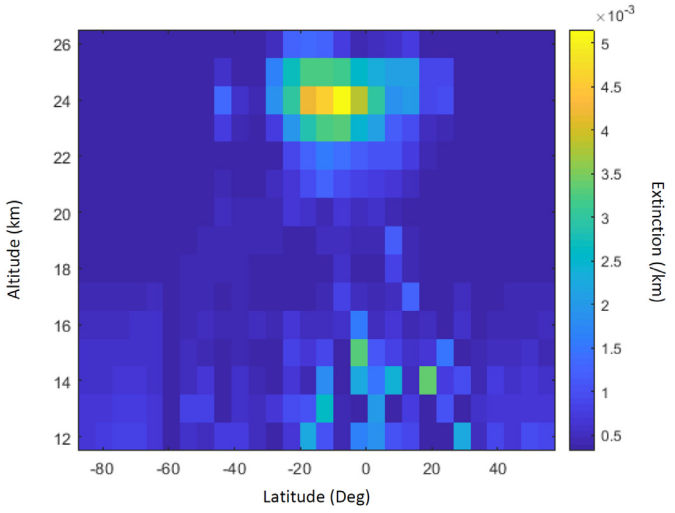


**Fig. 4.** Aerosol extinction for April 2022. ACE Imager aerosol extinction at 1.02 $\mu$m for 5° latitude by 1 km altitude bins.

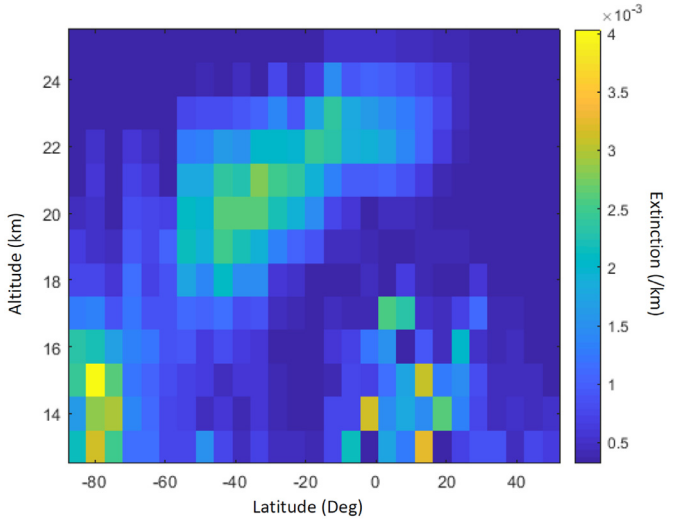


**Fig. 5.** Aerosol extinction for August 2022. ACE Imager aerosol extinction at 1.02 $\mu$m for 5° latitude by 1 km altitude bins.

test the generality of these correlations, points from the Raikoke [17] and 2011 Nabro [27] volcanic eruptions are included in Fig. 6. Note that Tonga points are mainly on the left of Fig. 6 and Raikoke points on the right: two overlapping data sets whose combination provides excellent coverage of the range of possible stratospheric conditions for sulfate aerosols. The retrieved properties from the Raikoke and Nabro volcanic plumes are provided in Supplementary Information Tables 2 and 3, respectively. As the temperature decreases and the water vapor pressure increases, the % sulfuric acid in the aerosol decreases, presumably a consequence of $H_2O$ taken up by the droplet. The dependence on temperature is particularly strong; Fig. 7 plots the composition of the Tonga plume as a function of temperature.

The points for the Tonga and Raikoke eruptions were fitted with a multiple linear regression model with temperature, $T$ in K, and water vapor pressure, $\log_{10}(P_{H2O})$ with $P_{H2O}$ in Pa, as independent variables and% sulfuric acid ($w_{H2SO4}$) as the dependent variable. Points from Tonga eruption from February 2022 and points from Raikoke eruption from July 2019 were excluded from the fit to allow time for rapid changes such as coagulation and chemistry to be finished after the eruption. The non-linear dependence of com-

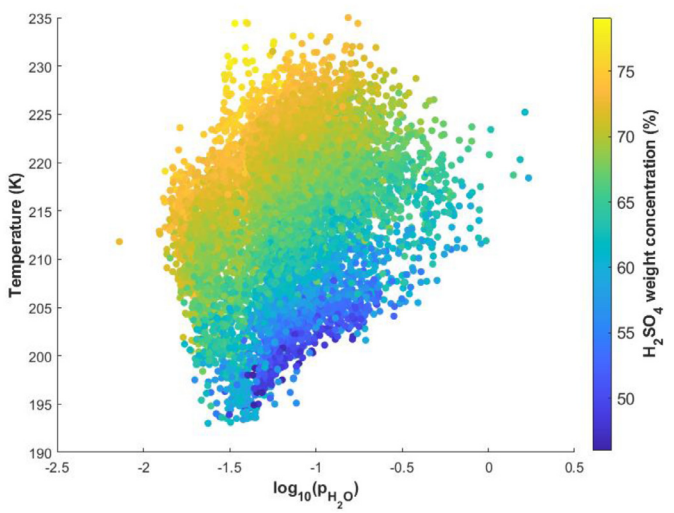


**Fig. 6.** Observed composition of sulfate aerosols. The $H_2SO_4$ concentration (weight %) using the color scale on the right as a function of temperature (K) and $\log_{10}(H_2O$ vapor pressure in Pa). As the temperature decreases and the water vapor pressure increases, the sulfuric acid concentration decreases. Points from Tonga, Raikoke and Nabro volcanic eruptions are included.

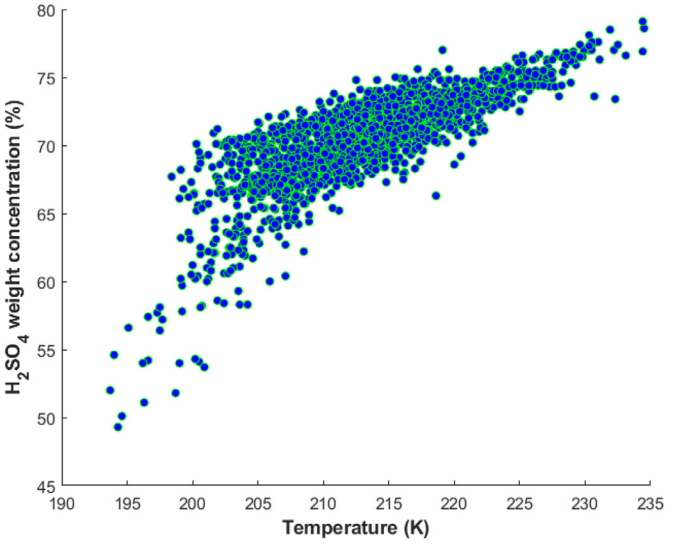


**Fig. 7.** Composition of Tonga aerosols. $H_2SO_4$ concentration (weight %) as a function temperature.

position on temperature (Fig. 7) was accounted for by adding a $T^2$ term to the model, and the model includes a cross term between the independent variables as well as between $\log_{10}(P_{H2O})$ and $T^2$. The fitted expression is:

$$w_{H_2SO_4} = -3247.97853 - 2006.27938 \cdot \log(p_{H_2O}) + 29.50612 \cdot T + 18.09112 \cdot \log(p_{H_2O}) \cdot T - 0.06570 \cdot T^2 - 0.04091 \cdot \log(p_{H_2O}) \cdot T^2 \quad (3)$$

The coefficient of determination statistic $R^2$ has a value of 0.88 and errors for the six fitting parameters are given as 95% confidence intervals in Table 1.

The strong dependence on temperature of aerosol composition is not unexpected because the vapor pressure of water is an exponential function of temperature (at equilibrium). Therefore as temperaure decreases, water vapor pressure decreases and more water will go into sulfate solution, diluting the $H_2SO_4$ concentration.

In contrast to the composition, the median radii, $r_m$, of the sulfate aerosols depend relatively weakly on temperature and wa-

**Table 1**
Model Fitting Parameters 95% confidence intervals for expression.

$W_{H2SO_4} = b_1 + b_2 \cdot \log(p_{H_2O}) + b_3 \cdot T + b_4 \cdot \log(p_{H_2O}) \cdot T + b_5 \cdot T^2 + b_6 \cdot \log(p_{H_2O}) \cdot T^2$

| $b_1$ | $b_2$ | $b_3$ | $b_4$ | $b_5$ | $b_6$ |
|---|---|---|---|---|---|
| −3247.978526 | −2006.279378 | 29.50611648 | 18.09111791 | −0.065698667 | −0.040907737 |
| | **b-lower margin** | **b-upper margin** | | | |
| $b_1$ | −3402.87290 | −3093.08416 | | | |
| $b_2$ | −2126.71903 | −1885.83972 | | | |
| $b_3$ | 28.06348 | 30.94875 | | | |
| $b_4$ | 16.96591 | 19.21632 | | | |
| $b_5$ | −0.06906 | −0.06234 | | | |
| $b_6$ | −0.04353 | −0.03828 | | | |

Note that the parameters are strongly correlated.

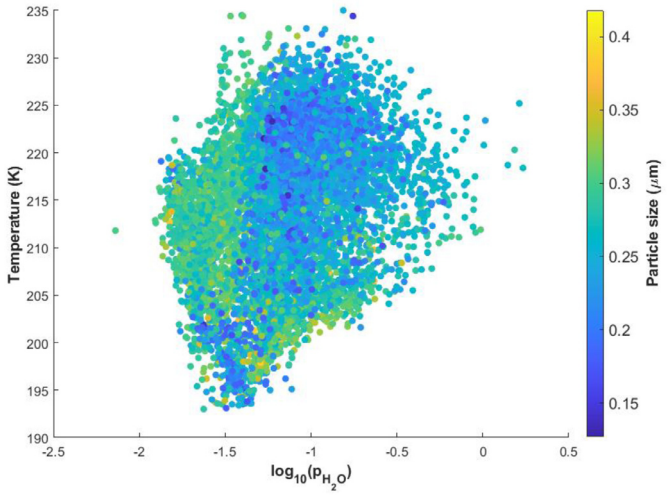


**Fig. 8.** Observed median particle radius. Particle size $r_m$ in $\mu$m as a function of temperature and logarithm (base 10) of the water vapor pressure in Pa.

ter vapor pressure (Fig. 8). The average value of $r_m$ for the Tonga plume is 0.295 ± 0.022 $\mu$m, with one standard deviation error bar. The values for Raikoke and Nabro are 0.257 ± 0.027 $\mu$m and 0.214 ± 0.031 $\mu$m, respectively. The median radii for Tonga and Raikoke are the same with error limits, but Nabro is smaller; combining all three data sets gives $r_m = 0.261 \pm 0.035$ $\mu$m.

Data from the Nabro volcanic plume were not included in the derivation of Eq. (3). As a test of its general applicability, the predictions for Nabro are included as Supplementary Information Table 4. The mean of the absolute values of observed and predicted composition differences, and the standard deviation is 1.0 ± 0.9% $H_2SO_4$ with outlying points (> 5.9% deviation) excluded. Therefore Eq. (3) can be used for the prediction of stratospheric sulfate aerosol composition in climate and chemical transport models for volcanic eruptions. The model works best for temperatures greater than 205 K.

There are thermodynamic predictions for the size and composition stratospheric sulfate aerosols [28,29]. The size of the aerosols depends on the mass of sulfuric acid in the droplet but depends only weakly (as we find, Fig. 8) on temperature and water vapor pressure for typical stratospheric conditions [29]. The composition at a given temperature depends only on the water vapor pressure and the predicted thermodynamic values are in reasonable agreement with our observations [29]. For three examples from Raikoke, the composition predictions [29] for 225 K, 220 K and 215 K are 72.4%, 69.4%, 68.1% compared to the observed 72.8%, 69.9% and 68.8%, respectively. Although our analysis and model are for volcanic plumes, the work is based on thermodynamic variables, so Eq. (3) likely applies to background stratospheric aerosols; further work on this topic with ACE data is underway.

## Declaration of Competing Interest

The authors declare that they have no known competing financial interests or personal relationships that could have appeared to influence the work reported in this paper.

## CRediT authorship contribution statement

**P. Bernath:** Conceptualization, Writing – original draft, Supervision. **C. Boone:** Conceptualization, Formal analysis, Software, Writing – review & editing. **A. Pastorek:** Formal analysis, Visualization, Writing – review & editing. **D. Cameron:** Formal analysis, Visualization, Writing – review & editing. **M. Lecours:** Data curation, Writing – review & editing.

## Data availability

ACE-FTS version 4.1/4.2 retrievals and atmospheric extinctions from the imagers are freely available (after registration). The data for Figs. 3, 6, 7, 8 are available as Supplementary Material.

## Acknowledgements

The ACE mission is funded by the Canadian Space Agency. Some support was also provided by NASA through the SAGE-III-ISS Science Team (80NSSC21K1194). PB acknowledges RB for productive discussion.

## Supplementary materials

Supplementary material associated with this article can be found, in the online version, at doi:10.1016/j.jqsrt.2023.108520.

## References

[1] Kremser S, et al. Stratospheric aerosol - observations, processes, and impact on climate. Rev Geophys 2016;54:278–335.
[2] Thompson DWJ, et al. Identifying signatures of natural climate variability in time series of global-mean surface temperature: methodology and insights. J Clim 2009;22:6120–41.
[3] Gleason JF, et al. Record low global ozone in 1992. Science 1993;260:523–6.
[4] Robock A. Volcanic eruptions and climate. Rev Geophys 2000;38:191–219.
[5] Persad GG, Samset BH, Wilcox LJ. Aerosols must be part of climate risk assessments. Nature 2022;611:662–4.
[6] Matoza RS, et al. Atmospheric waves and global seismoacoustic observations of the January 2022 Hunga eruption, Tonga. Sci 2022;377:95–100.
[7] Carr JL, Horváth K, Wu DL, Friberg MD. Stereo plume height and motion retrievals for the record-setting Hunga Tonga-Hunga Ha'apai eruption of 15 January 2022. Geophys Res Lett 2022;49 e2022GL098131.
[8] Proud SR, Prata A, Schmauss S. The January 2022 eruption of Hunga Tonga-Hunga Ha'apai volcano reached the mesosphere. Science 2022;378:554–7.
[9] Millán L, et al. The Hunga Tonga-Hunga Ha'apai hydration of the stratosphere. Geophys Res Lett 2022;49 e2002GL099381.

[10] Vömel H, Evan S, Tully M. Water vapor injection into the stratosphere by Hunga Tonga-Hunga Ha'apai. Science 2022;377:1444–7.
[11] Schoeberl MR, Wang Y, Ueyama R, Taha G, Jensen E, Yu W. Analysis and impact of the Hunga Tonga-Hunga Ha'apai stratospheric water vapor plume. Geophys Res Lett 2022;49 e2022GL100248.
[12] Coy L, Newman P, Wargan K, Partyka G, Strahan S, Pawson S. Stratospheric circulation changes associated with the Hunga Tonga-Hunga Ha'apai eruption. Geophys Res Lett 2022;49 e2022GL100982.
[13] Zhu Y, et al. Perturbations in stratospheric aerosol evolution due to the water-rich plume of the 2022 Hunga-Tonga eruption. Commun Earth Environ 2022;3:248.
[14] Kloss C, et al. Aerosol characterization of the stratospheric plume from the volcanic eruption at Hunga Tonga 15 January 2022. Geophys Res Lett 2022;49 e2022GL099394.
[15] Taha G, Loughman R, Colarco PR, Zhu T, Thomason LW, Jaross G. Tracking the 2022 Hunga Tonga-Hunga Ha'apai aerosol cloud in the upper and middle stratosphere using space-based observations. Geophys Res Lett 2022;49 e2022GL100091.
[16] Lacis A, Hansen J, Sato M. Climate forcing by stratospheric aerosols. Geophys Res Lett 1992;19:1607–10.
[17] Boone CD, Bernath PF, LaBelle K, Crouse J. Stratospheric aerosol composition observed by the atmospheric chemistry experiment following the 2019 Raikoke eruption. J Geophys Res 2022;127 e2022JD036600.
[18] Palmer KF, Williams D. Optical constants of sulfuric acid; application to the clouds of Venus? Appl Opt 1975;14:208–19.
[19] Pierce JR, et al. Efficient formation of stratospheric aerosol for climate engineering by emission of condensible vapor from aircraft. Geophys Res Lett 2010;37:L18805.
[20] Krishnamohan KS, Bala G, Cao L, Duan L, Caldeira K. The climatic effects of hygroscopic growth of sulfate aerosols in the stratosphere. Earth's Fut 2020;8 e2019EF001326.
[21] Bernath PF. The atmospheric chemistry experiment (ACE). J Quant Spectrosc Rad Transf 2017;186:3–16.
[22] Lecours MJ, Bernath PF, Sorensen JJ, Boone CD, Johnson RM, LaBelle K. Atlas of ACE spectra of clouds and aerosols. J Quant Spectrosc Rad Transf 2022;292:108361.
[23] Boone CD, Bernath PF, Cok D, Steffen J, Jones SC. Version 4 retrievals for the atmospheric chemistry experiment Fourier Transform Spectrometer (ACE-FTS) and Imagers. J Quant Spectrosc Rad Transf 2020;247:106939.
[24] Bernath PF, Steffen J, Crouse J, Boone CD. Sixteen-year trends in atmospheric trace gases from orbit. J Quant Spectrosc Rad Transf 2020;253:107178.
[25] Lecours M, Bernath P, Boone C, Crouse J. Infrared transmittance spectra of polar stratospheric clouds. J Quant Spectrosc Rad Transf 2023;294:108406.
[26] Lund Myhre CE, Christensen DH, Nicolaisen FM, Nielsen CJ. Spectroscopic study of aqueous $H_2SO_4$ at different temperatures and compositions: variations in dissociation and optical properties. J Phys Chem A 2003;107:1979–91.
[27] Cameron WD, Bernath P, Boone C. Sulfur dioxide from the Atmospheric Chemistry Experiment (ACE) satellite. J Quant Spectrosc Rad Transf 2020;258:107341.
[28] Carslaw KS, Simon L, Clegg SL, Brimblecombe P. A thermodynamic model of the system HCl-$HNO_3$-$H_2SO_4$-$H_2O$, including solubilities of HBr, from $<$200 to 328 K. J Phys Chem 1995;99:11557–74.
[29] Steele HM, Hamill P. Effects of temperature and humidity on the growth and optical properties of sulphuric acid-water droplets in the stratosphere. J Aerosol Sci 1981;12:517–28.